Extended Abstracts of the 2006 International Conference on Solid State Devices and Materials, Yokohama, 2006, pp. 124-125

F-1-3

Formation of Ferroelectric $Sr_2(Ta_{1-x},Nb_x)_2O_7$ Thin Film on Amorphous SiO_2 by Microwave-Excited Plasma Enhanced Metalorganic Chemical Vapor Deposition

Ichirou Takahashi, Kiyoshi funaiwa, Keita Azumi, Satoru Yamashita, Yasuyuki Shirai, Masaki Hirayama, Akinobu Teramoto, Shigetoshi Sugawa[1], and Tadahiro Ohmi
Phone: +81-22-217-3977 Fax: +81-22-217-3986 e-mail: ichirou@fff.niche.tohoku.ac.jp
New Industry Creation Hatchery Center, Tohoku University, Sendai 980-8579, Japan
[1]Graduate School of Engineering, Tohoku University, Sendai 980-8579, Japan

1. Introduction

$Sr_2(Ta_{1-x},Nb_x)_2O_7$ (STN) film is one of the most practical candidates for one-transistor-type ferroelectric memory devices, because it has a low dielectric constant and small remanent polarization [1]. However, since the ionization energy of Ta and Nb is very large, it is very difficult to oxidize them to pentad. As a result, another crystal phase such as $Sr(Ta_{1-x},Nb_x)O_3$ is easily formed. We have reported that 100 nm perovskite STN has been formed on SiO_2 by repeating the 5 nm STN sputtering deposition and oxygen radical treatment (oxidation of ferroelectric by the microwave-excited plasma) 20 times, and that 3 V operation of the MFIS structure device has been successfully achieved [2]. These results indicate that perovskite STN with high quality will be obtained by forming it in the plasma that has a large amount of radical oxygen. In this work, we report the newly developed microwave-excited (2.45 GHz) plasma enhanced metalorganic chemical vapor deposition (MOCVD) equipment. We also report the characteristics of the IrO_2/STN/SiO_2/P-type Si device.

2. Experimental

Figure 1 shows the newly developed MOCVD equipment. O_2 and plasma excitation gas such as Kr are introduced through upper shower nozzle. Metalorganic (MO) gas is introduced from lower nozzle into a diffusion plasma region whose electron temperature is below 1 eV. Figure 2 shows the schematic diagram of the gas supply system. To confirm the effect of the Kr/O_2 mixture plasma, the oxidation experiment of Si by the plasma was performed, as shown in Table Ⅰ. Gas line A is for Sr supply and $Sr(dpm)_2$ was used as a raw material. Gas line B is for Ta and Nb supply and $(Ta_{0.6},Nb_{0.4})(OEt)_5$ was used as a raw material. The condition of the STN formation is also shown in Table Ⅰ. Total working pressure was 66.6 Pa and microwave power was 1 KW. The composition of the STN film was evaluated by an inductively coupled plasma atomic emission spectrometry and $Sr_2(Ta_{0.76},Nb_{0.24})_2O_7$ was obtained.

3. Results and Discussions

Figure 3 shows XRD patterns of (a) STN (150 nm)/SiO_2 (sample A, without seed layer), (b) STN (140 nm)/10 nm STN seed layer/SiO_2 (sample B), and ferroelectric multilayer stack (FMLS)-STN (100 nm)/SiO_2 [2]. These films were formed by rf sputtering. In the case of the sample A, the pattern indicates the growth of a $Sr_3(Ta,Nb)_6Si_4O_{26}$ phase. On the other hand, in the case of the sample B, Both perovskite STN and $Sr_3(Ta,Nb)_6Si_4O_{26}$ are obtained. In the case of the FMLS-STN, the XRD patterns show that the peaks of $Sr_3(Ta,Nb)_6Si_4O_{26}$ cannot be observed at all and that perovskite STN is successfully fabricated. This indicates that in order to obtain perovskite STN with high quality it is effective to oxidize not only bottom part of STN (seed layer) but also whole STN film by oxygen radical treatment. On the basis of the results obtained, we developed microwave-excited plasma enhanced MOCVD equipment in which STN can be deposited in the radical oxygen atmosphere. Figure 4 shows the thickness of SiO_2 as a function of the mixing ratio of $O_2/(O_2 + Kr)$ flow rate that is introduced from upper shower nozzle. Plasma oxidation time is 10 minutes. When the ratio is from 0.1 to3%, the oxidation rate is large. This result shows that the most a large amount of radical oxygen has been generated at these ratios. Figures 5 and 6 show the thickness of SiO_2 as a function of microwave power and working pressure, respectively. Enlarging the power and lowering the working pressure promote the oxidation. Figure 7 shows Arrhenius plot on thickness of silicon oxide formed by the plasma oxidation and thermal oxidation. The results indicate that the mechanism of the plasma oxidation is completely different from that of thermal oxidation and that the oxidation is performed by radical oxygen. On the basis of these experimental results, the deposition condition of Sr_2O_2, $(Ta_{1-x}, Nb_x)_2O_5$, and STN was fixed, as shown in Table Ⅰ. Figure 8 shows the deposition rate of Sr_2O_2 and $(Ta_{1-x}, Nb_x)_2O_5$ as a function of the substrate temperature. The deposition rate of the plasma enhanced MOCVD dose not depend on the substrate temperature. Figure 10 shows XRD patterns of the fabricated films on SiO_2 by the plasma enhanced MOCVD. When the crystallization annealing temperature is 850℃, the XRD patterns indicate that $Sr(Ta_{1-x},Nb_x)O_3$ phase is fabricated. On the other hand, at the temperature of 950℃, the XRD patterns indicate that perovskite STN is obtained. Figure 11(a) and (b) show C-V characteristics of IrO_2/ STN (200 nm)/ SiO_2 (10 nm)/ Si device (as shown in Fig. 9) with the crystallization annealing of 850 and 950 ℃, respectively. At the temperature of 850℃, hysteresis in the CV curve is hardly obtained. On the other hand, at the temperature of 950℃, the device shows square hysteresis curves and a memory window of 1.2 V under 5 V writing operation. These results indicate that since newly developed MOCVD equipment can deposit ferroelectric film in the oxygen radical atmosphere, it is possible to fabricate ferroelectric STN on amorphous SiO_2. This technology can be well applied to MFIS-FET device formation.

4. Conclusion

We have successfully developed the microwave-excited plasma enhanced MOCVD equipment in which ferroelectric film can be deposited in the oxygen radical atmosphere. We have successfully fabricated perovskite STN on amorphous SiO_2 by the MOCVD for the first time. The fabricated MFIS structure device shows square hysteresis curves and a memory window of 1.2 V under 5 V writing operation.

References

[1] Y. Fujimori et al., Jpn. J. Appl. Phys., vol. 38, p. 2285 (1999)
[2] I. Takahashi et al, the abstract of the 17th International Symposium of Integrated Ferroelectric, 1-10-C (2005).

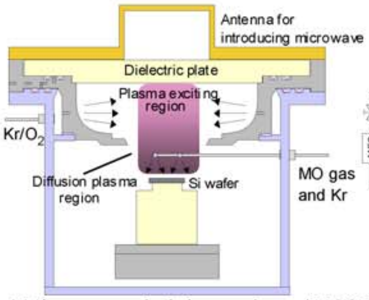

Fig.1 Microwave-excited plasma enhanced MOCVD equipment.

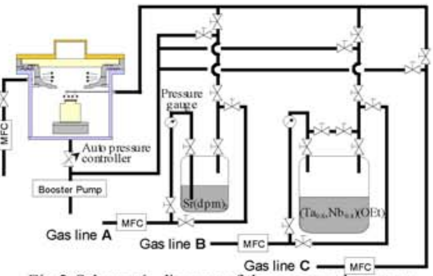

Fig.2 Schematic diagram of the gas supply system.

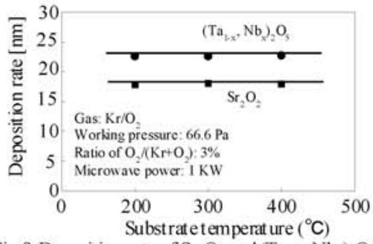

Fig.8 Deposition rate of Sr_2O_2 and $(Ta_{1-x}, Nb_x)_2O_5$ as a function of the substrate temperature.

Table Ⅰ Experimental conditions of the Microwave-excited plasma enhanced MOCVD system.

		Si oxidation		Sr_2O_2 deposition		(Ta, Nb)$_2$O$_5$ deposition		STN deposition	
		Gas	Flow rate [sccm]	Gas	Flow rate [sccm]	Gas	Flow rate [sccm]	Gas	Flow rate [sccm]
Gas supply	Upper shower nozzle	Kr O_2	500-x X(0.5～50)	Kr O_2	485 15	Kr O_2	485 15	Kr O_2	485 15
	MO shower nozzle: Gas line A	−	0	Kr	50	−	0	Kr	70
	MO shower nozzle: Gas line B	−	0	−	0	Kr	50	Kr	30
	MO shower nozzle: Gas line C	Kr	100	−	0	−	0	−	0
Plasma condition	Microwave power [KW]	0.5～1.0		1.0		1.0		1.0	
	Working pressure [Pa]	67～133		67		67		67	
Substrate temperature [℃]		200～400		400		400		400	

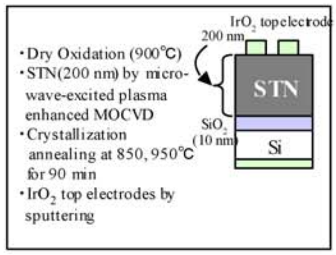

Fig.9 Device structure images and the process flows of the MFIS structure device formed by the microwave-excited plasma enhanced MOCVD.

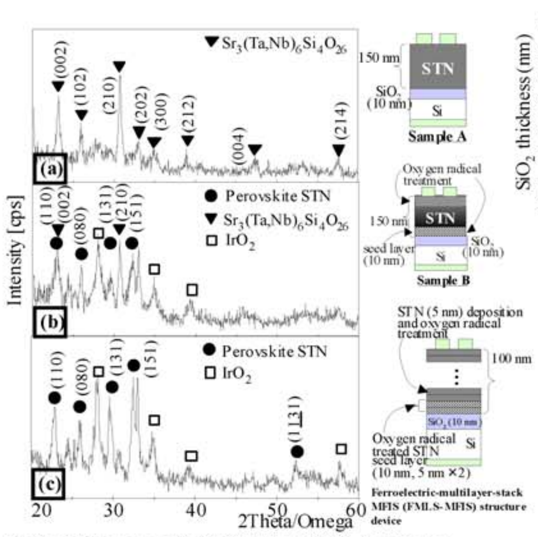

Fig.3 XRD patterns of (a)STN (150 nm)/SiO_2 (sample A), (b)STN (140 nm)/10 nm STN seed layer/SiO_2 (sample B), and (c) STN (100 nm)/SiO_2 formed by FMLS process [2].

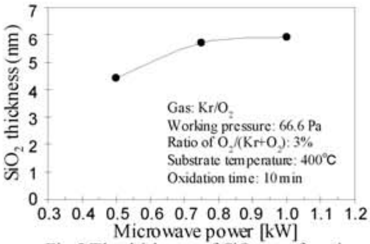

Fig.5 The thickness of SiO_2 as a function of microwave power.

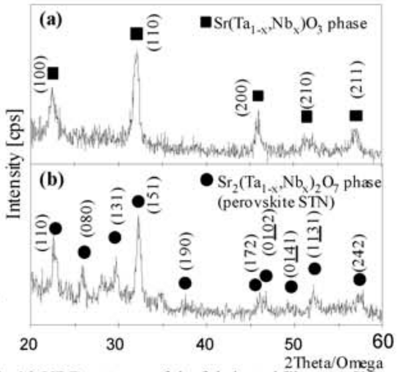

Fig.10 XRD patterns of the fabricated films on SiO_2 by the plasma enhanced MOCVD. Crystallization annealing temperature of (a) and (b) are 850 and 950 ℃, respectively.

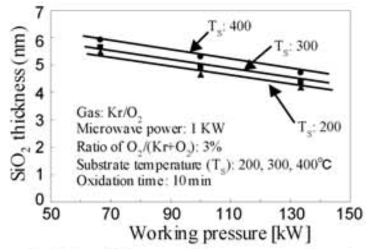

Fig.6 The thickness of SiO_2 as a function of working pressure.

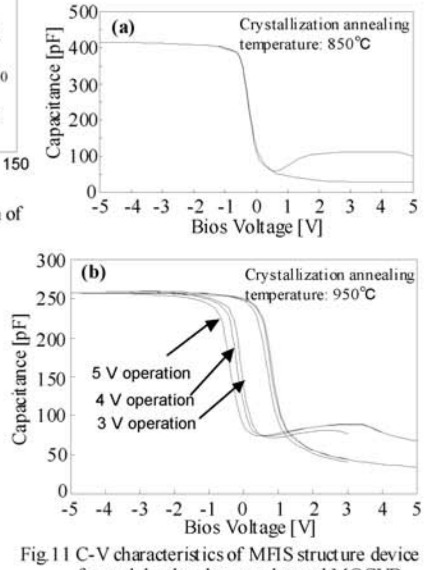

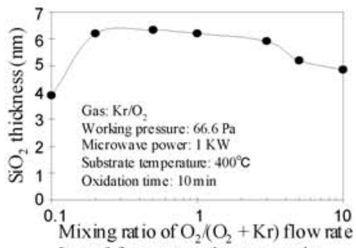

Mixing ratio of $O_2/(O_2+Kr)$ flow rate [sccm] from upper shower nozzle

Fig.4 The thickness of SiO_2 as a function of the mixing ratio of $O_2/(O_2+Kr)$ flow rate that is introduced from upper shower nozzle.

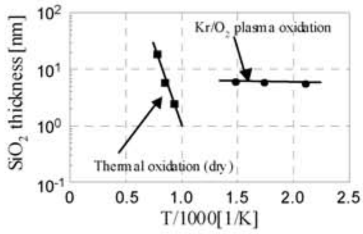

Fig.7 Arrhenius plot on thickness of silicon oxide.

Fig.11 C-V characteristics of MFIS structure device formed by the plasma enhanced MOCVD. Crystallization annealing temperature of (a) and (b) are 850 and 950 ℃, respectively.